

# A Comparison of Gaussian and Fourier Methods for Degenerate Diffusions on SE(2)

Hui Dong<sup>1</sup> and Gregory S. Chirikjian<sup>2</sup>

**Abstract**—Degenerate diffusions on the special Euclidean group of the plane arise in a number of applications in filtering theory such as the construction of dead-reckoning priors in nonholonomic mobile robot pose estimation, and in inpainting and stochastic completion in the study of visual perception. Two very different solution methodologies have been pursued in the literature: (1) Gaussian distributions in exponential coordinates for very concentrated probability densities; (2) noncommutative Fourier expansions for very distributed probability densities. Here we compare and contrast these methodologies and examine the range over which they provide comparable answers and quantitatively analyze when one should be used over the other.

## I. INTRODUCTION

This paper compares two methods for constructing time-evolving probability densities of the form  $f(x, y, \theta; t)$  that solve degenerate diffusions on  $SE(2)$ , the group of rigid-body motions of the plane. The two solution methodologies that we compare are: (1) a generalized of Fourier solution; (2) a Gaussian solution in the exponential coordinates for this group.

Before going into technical details, we first consider a simple analogy to illustrate the motivation for this work. The diffusion equation with drift on the circle is of the form

$$\frac{\partial f}{\partial t} = \frac{1}{2} D \frac{\partial^2 f}{\partial \theta^2} - \omega \frac{\partial f}{\partial \theta} \quad (1)$$

where  $D > 0$  is a diffusion constant, and  $\omega$  is a constant drift speed, which can take any real value. The solution to this equation subject to the initial conditions  $f(\theta; 0) = \delta(\theta - 0)$  (the Dirac delta function) can be written exactly in two very different ways:

$$\begin{aligned} f(\theta; \mu, \sigma^2) &= \frac{1}{\sqrt{2\pi}\sigma} \sum_{k=-\infty}^{\infty} e^{-\frac{1}{2} \frac{(\theta-\mu-2\pi k)^2}{\sigma^2}} \\ &= \frac{1}{2\pi} + \frac{1}{\pi} \sum_{n=1}^{\infty} e^{-\frac{\sigma^2}{2} n^2} \cos(n(\theta - \mu)) \end{aligned} \quad (2)$$

<sup>1</sup>Hui Dong is with the School of Mechanical Engineering and Automation, Fuzhou University, Fuzhou, China. d.hui.hit@gmail.com

<sup>2</sup>Gregory S. Chirikjian is with the Department of Mechanical Engineering, The Johns Hopkins University, Baltimore, MD 21218 USA. gregc@jhu.edu

where  $\sigma^2 = Dt$  and  $\mu = \omega t \bmod 2\pi$ . The first of these is a “wrapped Gaussian” or “folded normal” distribution where the solution on the real line has been made into a  $2\pi$ -periodic function (i.e., a “function on the circle”). In the second equality, this periodic function has been expressed as a Fourier series. As  $\sigma^2$  becomes small, we can truncate the summation over  $k$  at  $k = 0$  because the tails of the Gaussian decay rapidly. In the second solution, when  $\sigma^2$  is large, we can truncate at  $|n| = 1$  as the distribution becomes a small perturbation on the uniform distribution on the circle.

Analogous solution methodologies exist for more complicated scenarios. In particular, degenerate diffusions<sup>1</sup> on the proper group of motions of the Euclidean plane, also called the “special Euclidean group”,  $SE(2)$ , arise in a surprising number of distinct application areas. Unlike in the Euclidean case, diffusions on Lie groups with degenerate diffusion matrices can result in probability densities that are well behaved.

Applications of these degenerate diffusions on  $SE(2)$  include modeling dead-reckoning errors in mobile robot pose estimation [17], [24], [34], stochastic completion and inpainting in image analysis [13], [14], [31], [15], [35], visual perception [4], [5], [11], [12], [16], [21], and phase noise in optical communications [30]. And 3D analogs of these result in applications as diverse as DNA statistical mechanics [33] and steering of flexible needles [23]. Our motivation is mobile robot dead-reckoning models, but the methodological developments are applicable to all of the above.

Here we compare the range of applicability of Fourier and Gaussian solutions in these scenarios.

Let

$$g(x, y, \theta) \doteq \begin{pmatrix} \cos \theta & -\sin \theta & x \\ \sin \theta & \cos \theta & y \\ 0 & 0 & 1 \end{pmatrix} \quad (3)$$

denote the homogeneous transformation matrix describing rigid-body transformations in the plane (with translation parameterized using Cartesian coordinates). The

<sup>1</sup>These are diffusions with drift in multiple directions such that the diffusion matrix is positive semi-definite instead of positive definite.

set of all such positions and orientations (or poses) is called  $SE(2)$ . This is an example of a Lie group under the operation of matrix multiplication. That is,  $g_1 \circ g_2 \doteq g(x_1, y_1, \theta_1)g(x_2, y_2, \theta_2)$ . The group identity is  $e = g(0, 0, 0)$ , and the existence of an inverse for each element and the associative law  $(g_1 \circ g_2) \circ g_3 = g_1 \circ (g_2 \circ g_3)$  all follow from the fact that  $SE(2)$  is a matrix Lie group. This is an example of a noncommutative group since  $g_1 \circ g_2 \neq g_2 \circ g_1$ .

It is also possible to use polar coordinates for translations:  $x = r \cos \phi$  and  $y = r \sin \phi$ . The space of all poses is parameterized by  $(x, y, \theta) \in \mathbb{R} \times \mathbb{R} \times \mathbb{S}^1$ , or equivalently  $(r, \phi, \theta) \in \mathbb{R}_{\geq 0} \times \mathbb{S}^1 \times \mathbb{S}^1$ . It is possible to integrate functions on this space as

$$\begin{aligned} \int_{SE(2)} f(g) dg &\doteq \int_{-\pi}^{\pi} \int_{-\infty}^{\infty} \int_{-\infty}^{\infty} f(x, y, \theta) dx dy d\theta \\ &= \int_{-\pi}^{\pi} \int_{-\pi}^{\pi} \int_0^{\infty} f(r, \phi, \theta) r dr d\phi d\theta. \end{aligned}$$

Consider a kinematic cart which executes noisy trajectories, as shown in Fig. 1. Each of the two wheels have a desired rotational rate of  $v$ , and so the infinitesimal angle that each wheel would turn through at time  $t$  is  $d\phi_i(t) = vdt$ . Superimposed on each of these wheel motions white noise (increments of a Wiener process),  $d\phi_i(t) = v dt + \sqrt{D} dw_i$ . Substituting this into the nonholonomic equations for the kinematic cart gives the following model for dead-reckoning errors in mobile robotics [34]:

$$\begin{aligned} \begin{pmatrix} dx \\ dy \\ d\theta \end{pmatrix} &= \begin{pmatrix} r_w v \cos \theta \\ r_w v \sin \theta \\ 0 \end{pmatrix} dt \\ &+ \sqrt{D} \begin{pmatrix} \frac{r_w}{2} \cos \theta & \frac{r_w}{2} \cos \theta \\ \frac{r_w}{2} \sin \theta & \frac{r_w}{2} \sin \theta \\ \frac{r_w}{l} & -\frac{r_w}{l} \end{pmatrix} \begin{pmatrix} dw_1 \\ dw_2 \end{pmatrix}, \end{aligned} \quad (4)$$

where  $r_w$  is the radius of both of the cart's wheels and  $l$  is the length of cart axle. This is a stochastic differential equation (SDE). Usually two kinds (or interpretations) of SDEs are used to model systems: Ito or Stratonovich. It can be shown that the particular SDE in (4) is a special case in which it does not matter which interpretation is used. Closely related models include those used in [2], [28], [3], [18], [19], [20], [26]. Corresponding to every SDE is a diffusion equation that generates the same probability density that would result from running an infinite number of random trials of the SDE. This is

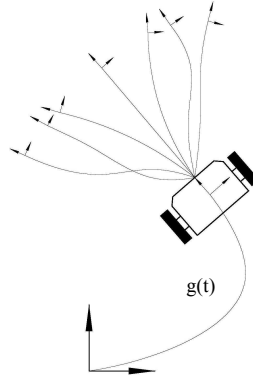


Fig. 1. A kinematic cart with an uncertain future position and orientation

called the Fokker-Planck equation (FPE), and the FPE corresponding to the SDE in (4) is

$$\begin{aligned} \frac{\partial f(g, t)}{\partial t} &= -r_w v \tilde{X}_1 f \\ &+ \frac{D}{2} \left[ \frac{r_w^2}{2} \left( \tilde{X}_1 \right)^2 + \frac{2r_w^2}{l^2} \left( \tilde{X}_3 \right)^2 \right] f. \end{aligned} \quad (5)$$

where

$$\tilde{X}_1 = \cos \theta \frac{\partial}{\partial x} + \sin \theta \frac{\partial}{\partial y} \quad (6)$$

$$\tilde{X}_2 = -\sin \theta \frac{\partial}{\partial x} + \cos \theta \frac{\partial}{\partial y} \quad (7)$$

$$\tilde{X}_3 = \frac{\partial}{\partial \theta} \quad (8)$$

are a basis for all left-invariant vector fields on  $SE(2)$ .

Equation (5) is an example of a more general equation of the form

$$\frac{\partial f}{\partial t} = \left( - \sum_{i=1}^3 h_i(t) \tilde{X}_i + \frac{1}{2} \sum_{i,j=1}^3 D_{ij}(t) \tilde{X}_i \tilde{X}_j \right) f \quad (9)$$

where  $f = f(g, t)$  and the coefficient matrix  $D(t)$  is symmetric and positive semi-definite. When  $\det D = 0$ , and at least one eigenvalue is non-negative, this is the degenerate case. And often in applications  $h(t)$  and  $D(t)$  are constant.

It is possible to solve (5) subject to the initial conditions  $f(g; 0) = \delta(g) \doteq \delta(x - 0)\delta(y - 0)\delta(\theta - 0)$  using either Fourier methods or Gaussian approaches, in analogy with diffusions on the circle.

The remainder of this paper is structured as follows. Section II explains how operational properties of the Fourier transform on  $SE(2)$  can be used to solve these sorts of degenerate diffusions. Section III derives a Gaussian solution. Section IV examines the solutions

in the case when only one of the three directions of infinitesimal motion has nonzero diffusion coefficient. And Section V computes the Gaussian and Fourier solutions numerically and calculates their relative error.

## II. FOURIER SOLUTION

The Fourier transform on SE(2) is defined as [9], [10]

$$F(f) = \hat{f}(p) = \int_{SE(2)} f(g)U(g^{-1}, p)d(g) \quad (10)$$

and its inverse transform is defined as [9], [10]

$$F^{-1}(\hat{f}) = f(g) = \int_0^\infty \text{trace}(\hat{f}(p)U(g, p))pd(p) \quad (11)$$

where  $g$  denotes a member of SE(2),  $p$  is the “frequency” introduced by the Fourier transform, and  $U(g, p)$  is an irreducible unitary representation matrix of SE(2). Here the elements of matrix  $U(g, p)$  are given as [9], [10]

$$u_{mn}(g(r, \phi, \theta), p) = i^{n-m} e^{-i[n\theta + (m-n)\phi]} J_{n-m}(pr), \quad (12)$$

where  $-\infty < m, n < \infty$ , and  $g$  is used to describe the matrix form of cart motion in the plane (translation and rotation). An important operational property of the Fourier transform for SE(2) is

$$F(\tilde{X}_i f) = \eta_i(p) \hat{f}(p) \quad (13)$$

where  $\eta_i(p)$ ’s are coefficient matrices with elements [9], [10]

$$\eta_{1mn}(p) = \frac{p}{2}(\delta_{m,n+1} - \delta_{m,n-1}), \quad (14)$$

$$\eta_{2mn}(p) = \frac{ip}{2}(\delta_{m,n+1} + \delta_{m,n-1}), \quad (15)$$

$$\eta_{3mn}(p) = -im\delta_{m,n}, \quad (16)$$

where  $\delta$  is the Kronecker delta function. Note that in our context  $f = f(g, t)$  and  $\hat{f} = \hat{f}(p, t)$  – the time variable is unaffected by Fourier transformation on the group.

By applying the SE(2) Fourier transform on both sides of equation (5), we obtain

$$\frac{\partial \hat{f}}{\partial t} = (-r_w v \eta_1(p) + \frac{D}{2}(\frac{r_w^2}{2}\eta_1(p)^2 + \frac{2r_w^2}{l^2}\eta_3(p)^2))\hat{f}. \quad (17)$$

The solution to (5) is

$$\hat{f}(p, t) = \exp(A(p)t)\hat{f}(p, 0), \quad (18)$$

where

$$A(p) = -r_w v \eta_1(p) + \frac{D}{2} \left( \frac{r_w^2}{2}\eta_1(p)^2 + \frac{2r_w^2}{l^2}\eta_3(p)^2 \right), \quad (19)$$

and  $\exp$  is the matrix exponential. When  $t = 0$ , the initial condition for (5) is defined as

$$f(g(x, y, \theta); t = 0) = \delta(x)\delta(y)\delta(\theta), \quad (20)$$

where  $\delta$  is the Dirac delta function. As a result,  $\hat{f}(p, 0)$  is the identity matrix, and (18) is reduced to

$$\hat{f}(p, t) = \exp(A(p)t). \quad (21)$$

From this Fourier-space solution  $f(g, t)$  is obtained by applying the inverse Fourier transform in (11).

## III. GAUSSIAN SOLUTION

Whereas Cartesian coordinates in translation/position are convenient to state the original stochastic differential equation, and polar coordinates are convenient to use the SE(2) Fourier transform, a third set of coordinates: the exponential coordinates are most convenient to define Gaussian solutions. A basis for the Lie algebra  $se(2)$  is

$$X_1 = \begin{pmatrix} 0 & 0 & 1 \\ 0 & 0 & 0 \\ 0 & 0 & 0 \end{pmatrix};$$

$$X_2 = \begin{pmatrix} 0 & 0 & 0 \\ 0 & 0 & 1 \\ 0 & 0 & 0 \end{pmatrix};$$

$$X_3 = \begin{pmatrix} 0 & -1 & 0 \\ 1 & 0 & 0 \\ 0 & 0 & 0 \end{pmatrix}.$$

These respectively correspond to infinitesimal translations along the x and y axes, and rotation around the z axis and are related to  $\tilde{X}_i$  in (6)-(8) by

$$(\tilde{X}_i f)(g) := \left. \frac{d}{dt} f(g \circ \exp(tX_i)) \right|_{t=0}.$$

If  $X \doteq v_1 X_1 + v_2 X_2 + \alpha X_3$ , then rigid-body motions can be parameterized as

$$\begin{aligned} \tilde{g}(v_1, v_2, \alpha) &= \exp(v_1 X_1 + v_2 X_2 + \alpha X_3) \\ &= \exp \begin{pmatrix} 0 & -\alpha & v_1 \\ \alpha & 0 & v_2 \\ 0 & 0 & 0 \end{pmatrix}. \end{aligned}$$

This can be expressed in the closed form

$$\tilde{g}(v_1, v_2, \alpha) = \begin{pmatrix} \cos \alpha & -\sin \alpha & [v_2(-1 + \cos \alpha) + v_1 \sin \alpha]/\alpha \\ \sin \alpha & \cos \alpha & [v_1(1 - \cos \alpha) + v_2 \sin \alpha]/\alpha \\ 0 & 0 & 1 \end{pmatrix}.$$

The opposite of the matrix exponential is the matrix logarithm, which is well defined as long as  $|\alpha| \neq \pi$ . We also use the notation

$$(v_1 X_1 + v_2 X_2 + \alpha X_3)^\vee = [v_1, v_2, \alpha]^T.$$

Here we use  $\tilde{g}$  to distinguish this from the parameterization in (3).

Using these concepts, the mean of any probability density on  $SE(2)$  can be written as

$$\int_G \log^\vee(\mu^{-1}g) f(g) dg = \mathbf{0}. \quad (22)$$

This concept of mean, should not be confused with other related concepts presented recently in the literature. The above definition has some particularly useful properties for our application, as described below.

The covariance matrix  $\Sigma$  can be defined as

$$\Sigma = \int_G \log^\vee(\mu^{-1}g) (\log^\vee(\mu^{-1}g))^T f(g) dg. \quad (23)$$

And when  $\|\Sigma\| \ll 1$  a Gaussian distribution can be defined as

$$f(g; \mu, \Sigma) = \frac{1}{c(\Sigma)} \exp \left( -\frac{1}{2} [\log^\vee(\mu^{-1}g)]^T \Sigma^{-1} \log^\vee(\mu^{-1}g) \right). \quad (24)$$

Here  $c(\Sigma)$  is a normalizing factor that ensures that  $f(g; \mu, \Sigma)$  is a pdf. When the covariance is small this normalizing factor can be approximated as

$$c(\Sigma) \approx (2\pi)^{n/2} |\det(\Sigma)|^{1/2}$$

Suppose that  $f_i(g) = f(g; \mu_i, \Sigma_i)$ . Then the convolution is defined as

$$(f_1 * f_2)(g) = \int_{SE(2)} f_1(h) f_2(h^{-1} \circ g) dh.$$

It has been shown previously that the mean and covariance of concentrated distributions propagate under convolution as

$$\mu_{1*2} = \mu_1 \circ \mu_2 \text{ and } \Sigma_{1*2} = Ad(\mu_2^{-1}) \Sigma_1 Ad^T(\mu_2^{-1}) + \Sigma_2.$$

That is, these are the mean and covariance of  $(f_1 * f_2)(g)$ . The adjoint matrix is of the form

$$Ad(g(x, y, \theta)) = \begin{pmatrix} \cos \theta & -\sin \theta & y \\ \sin \theta & \cos \theta & -x \\ 0 & 0 & 1 \end{pmatrix}.$$

It has the properties

$$Ad(g_1 \circ g_2) = Ad(g_1) Ad(g_2)$$

$$Ad(g^{-1}) = Ad^{-1}(g)$$

$$Ad(e) = \mathbb{I}.$$

The above formulas can be iterated. For example, the mean and covariance of  $(f_1 * f_2) * f_3$  will be

$$\mu_{(1*2)*3} = (\mu_{1*2}) \circ \mu_3 = (\mu_1 \circ \mu_2) \circ \mu_3$$

and

$$\Sigma_{(1*2)*3} = Ad(\mu_3^{-1}) \Sigma_{1*2} Ad^T(\mu_3^{-1}) + \Sigma_3.$$

Iterating this formula, and removing the parenthesis (which are unnecessary due to the associativity of the group operation and the convolution operator),

$$\mu_{1*2*...*n} = \mu_1 \circ \mu_2 \circ \dots \circ \mu_n = \prod_{i=1}^n \mu_i \quad (25)$$

(where the order of multiplication in this product matters) and

$$\Sigma_{1*2*...*n} = \sum_{i=1}^n Ad^{-1} \left( \prod_{j=i+1}^n \mu_j \right) \Sigma_i Ad^{-T} \left( \prod_{j=i+1}^n \mu_j \right).$$

In the continuous time case, where each  $f_i(g)$  is replaced by an  $f_{\Delta t}(g)$ , then with initial conditions  $\mu(0) = e$  we get the product integral

$$\mu(t) = \bigcap_{0 \leq \tau \leq t} \exp \left( \sum_{i=1}^3 h_i(\tau) X_1 \right). \quad (26)$$

In some special cases this product integral becomes easy to compute in closed form. For example, if  $h_i$  is constant then

$$\mu(t) = \exp \left( t \sum_{i=1}^3 h_i X_1 \right).$$

Or if  $h_i(t) = h(t)c_i$  where  $c_i$  is constant, then

$$\mu(t) = \exp \left( \int_0^t h(t) dt \sum_{i=1}^3 c_i X_1 \right).$$

With initial conditions on the covariance  $\Sigma(0) = \mathbb{O}$ , and in the special case when  $\mu(t)$  follows a one-dimensional subgroup with constant speed, then

$$\Sigma(t) = \int_0^t Ad^{-1}(\mu(t-\tau)) D(t) Ad^T(\mu(t-\tau)) d\tau \quad (27)$$

because

$$\begin{aligned} Ad^{-1}(\mu(t)) Ad(\mu(\tau)) &= Ad(\mu^{-1}(t)) Ad(\mu(\tau)) \\ &= Ad(\mu^{-1}(t) \circ \mu(\tau)) = Ad^{-1}(\mu(t-\tau)). \end{aligned}$$

#### IV. THE SINGULAR CASE

Note that in (1), if the initial conditions are  $f(\theta, 0) = \delta(\theta)$ , and if  $D = 0$ , then the solution will simply be  $f(\theta, 0) = \delta(\theta - vt)$ . But in the case of degenerate diffusions on noncommutative Lie groups, it is not necessarily the case that the covariance matrix will have a zero eigenvalue just because the diffusion matrix does. This is because in (27) the  $Ad(\cdot)$  matrix can “mix” the diffusion coefficients in a way that leads to a nonsingular covariance.

Nevertheless, there are application areas such as stochastic completion and inpainting in image analysis

[13], [14], [31], [15], [35], visual perception [4], [5], [11], [12], [21], and phase noise in optical communications [30], in which the diffusion equation has a diffusion coefficient even more singular than the kinematic cart with noise.

In such equations the Fokker-Planck equation is of the form

$$\frac{\partial f(g, t)}{\partial t} = \left[ v\tilde{X}_1 + \frac{1}{2}D(\tilde{X}_3)^2 \right] f(g, t). \quad (28)$$

In this case

$$\mu(t) = \begin{pmatrix} 1 & 0 & vt \\ 0 & 1 & 0 \\ 0 & 0 & 1 \end{pmatrix}$$

and

$$D(t) = \begin{pmatrix} 0 & 0 & 0 \\ 0 & 0 & 0 \\ 0 & 0 & D \end{pmatrix}.$$

Using (27) in this case gives

$$\Sigma(t) = 0 \oplus \Sigma_{2 \times 2}(t).$$

This degeneracy of the Gaussian solution can be regularized by substituting a small positive constant value,  $\epsilon$ , in place of the zero in the above expression for  $\Sigma(t)$ . In contrast Fourier solution has a built-in mechanism for regularization, which is truncation of the infinite-dimensional Fourier matrices at finite size. This is somewhat like approximating a classical Dirac delta with a *sinc* function.

Instead of a regularized solution, it is possible to construct one in this case that is based on the Gaussian solution but retains the singular nature. In particular,

$$f(g; t) = \frac{1}{2\pi|\Sigma_{2 \times 2}(t)|^{\frac{1}{2}}} \delta(\mathbf{e}_1 \cdot \log^\vee(\mu^{-1}(t) \circ g)) \cdot \exp\left(-\frac{1}{2}[\log^\vee(\mu^{-1}(t) \circ g)]_2^T \Sigma_{2 \times 2}^{-1}(t) [\log^\vee(\mu^{-1}(t) \circ g)]_2\right) \quad (29)$$

where  $[\log^\vee(\mu^{-1}(t) \circ g)]_2$  denotes the two-dimensional vector consisting of the last two entries of  $\log^\vee(\mu^{-1}(t) \circ g)$ .

## V. NUMERICAL COMPARISON

We set  $h_1 = r_w\nu$ ,  $h_2 = 0$ ,  $h_3 = 0$ , so

$$\mu(t) = \begin{pmatrix} 1 & 0 & r_w\nu t \\ 0 & 1 & 0 \\ 0 & 0 & 1 \end{pmatrix}.$$

And comparing (5) and (9) we see that

$$D(t) = \begin{pmatrix} \frac{Dr_w^2}{2} & 0 & 0 \\ 0 & 0 & 0 \\ 0 & 0 & \frac{2Dr_w^2}{l^2} \end{pmatrix}$$

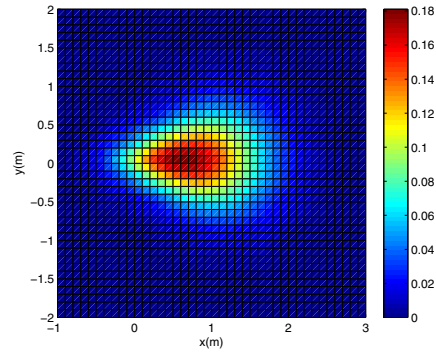


Fig. 2. Degenerate Diffusions Using Fourier Methods

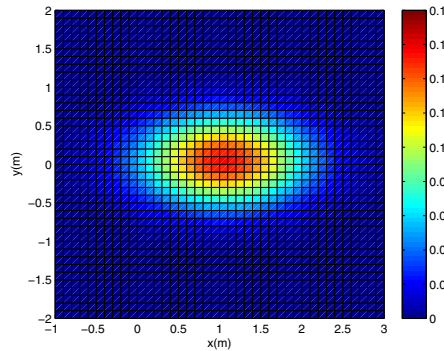


Fig. 3. Degenerate Diffusions as a Gaussian

(which is constant).

Substitute these into (27) and calculate  $\Sigma(t)$  in closed form

$$\Sigma(t) = \begin{pmatrix} \frac{Dr_w^2 t}{2} & 0 & 0 \\ 0 & \frac{2Dr_w^4 t^3 \nu^2}{3l^2} & \frac{Dr_w^3 t^2 \nu}{l^2} \\ 0 & \frac{Dr_w^3 t^2 \nu}{l^2} & \frac{2Dr_w^2 t}{l^2} \end{pmatrix}$$

Then, since  $\mu(t)$  and  $\Sigma(t)$  are known, evaluate (24) with  $\mu(t = 1)$  and  $\Sigma(t = 1)$ . Comparison the results of the SE(2) Fourier solution and Gaussian solution under the same conditions are shown in Fig.2-Fig.3 ,when  $D = r_w = t = v = l = 1, \theta = 0$ . Since the matrix  $U$  is infinite dimensional, we must truncate it to finite dimension as  $(2L + 1)$  by  $(2L + 1)$  matrices when doing numerical computations, where  $L = 4$ .  $p$  is the frequency introduced by the Fourier transform. We truncate it from 0 to 20 in the numerical computations.

TABLE I  
THE ERRORS BETWEEN THE GAUSSIAN AND FOURIER  
DESCRIPTIONS WITH DIFFERENT  $D$

$D$	$E_{error}$
0.1	0.1376
0.25	0.2469
0.5	0.3041
1	0.3216
1.5	0.3046
2	0.3181

The error is

$$E_{error} = \sqrt{\frac{\int_x \int_y (f_1(x, y, 0) - f_2(x, y, 0))^2 dx dy}{\int_x \int_y (f_1(x, y, 0))^2 dx dy}},$$

where  $f_1$  is the PDFs of dead-reckoning errors obtained from Fourier method,  $f_2$  is the PDFs from Gaussian method. The errors between the Gaussian and Fourier methods for different values of  $D$  are shown in Table.I.

We also compute the overall position error by computing

$$\tilde{f}_i(x, y) = \frac{1}{2\pi} \int_{-\pi}^{\pi} f_i(x, y, \theta) d\theta$$

and evaluating

$$\tilde{E}_{error} = \sqrt{\frac{\int_x \int_y (\tilde{f}_1(x, y) - \tilde{f}_2(x, y))^2 dx dy}{\int_x \int_y (\tilde{f}_1(x, y))^2 dx dy}},$$

The plots of  $\tilde{f}_i(x, y)$  are Fig.4 and Fig.5 We can see the errors results in Table.II.

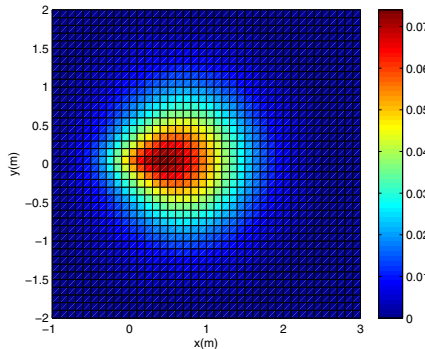


Fig. 4. Fourier Description of  $\tilde{f}_i(x, y)$

The probability of the real robot's location is dependant on  $D$ . Using both methods, we compare the probability density of the point  $(\tilde{r}, \tilde{\theta}) = (1, 0)$ , which is what the real robot's location would be if it were not noisy. The results are shown in the Table.III.

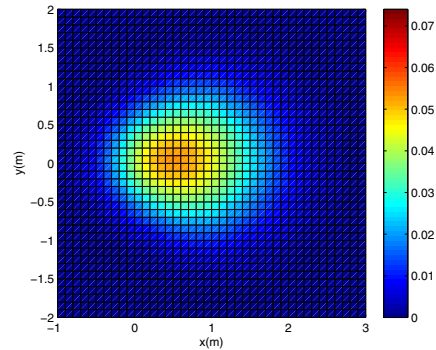


Fig. 5. Gaussian Description of  $\tilde{f}_i(x, y)$

TABLE II  
THE ERRORS BETWEEN THE GAUSSIAN AND FOURIER  
DESCRIPTIONS WITH DIFFERENT  $D$

$D$	$\tilde{E}_{error}$
0.1	0.1282
0.25	0.2869
0.5	0.2342
1	0.1869
1.5	0.2349
2	0.2883

TABLE III

PROBABILITY DENSITY EVALUATED AT THE ROBOT'S TARGET  
LOCATION COMPUTING BY GAUSSIAN AND FOURIER METHODS

$D$	Gaussian method	Fourier method
0.1	4.92	4.78
0.25	1.24	1.31
0.5	0.44	0.47
1	0.16	0.18
1.5	0.085	0.098
2	0.055	0.064

## VI. CONCLUSIONS

We present a comparison of Gaussian and Fourier methods for degenerate on  $SE(2)$  in this paper. The stochastic differential equations (SDEs) of dead-reckoning errors in mobile robotics are solved by the two methods. Plots of the solutions show them to be qualitatively similar. But as the diffusion parameter increases, the mean of the Gaussian solution appears to travel too far relative to that of the Fourier solution, leading to increasing errors. We believe that improvements can be made to (25) to make these solutions match better over a wider range of diffusion constants.

## REFERENCES

- [1] P-A Absil, R. Mahony, and R. Sepulchre. Optimization algorithms on matrix manifolds. Princeton University Press, 2009.
- [2] Barfoot, T.D., Furgale, P.T., “Associating Uncertainty with Three-Dimensional Poses for use in Estimation Problems,” *IEEE Transactions on Robotics*, 2014 (to appear)
- [3] Barrau, A., Bonnabel S., Invariant Particle Filtering with application to localization 53rd IEEE Conference on Decision and Control December 15-17, 2014. Los Angeles, California, USA 5599-5605
- [4] Boscain, U., Duplaix, J., Gauthier, J. P., Rossi, F., “Anthropomorphic image reconstruction via hypoelliptic diffusion,” *SIAM Journal on Control and Optimization*, 50(3):1309-1336, 2012.
- [5] Boscain, U., Chertovskih, R.A., Gauthier, J.P., Remizov, A.O., “Hypoelliptic Diffusion and Human Vision: A Semidiscrete New Twist,” *SIAM Journal on Imaging Sciences*, 7(2):669-695, 2014.
- [6] Bonnabel, S. , Martin, P., and Salaun, E., Invariant Extended Kalman Filter: Theory and Application to a Velocity-Aided Attitude Estimation Problem, Proc. of the 48th IEEE Conf. on Decision and Control, pp.1297-1304, 2009.
- [7] Bourmaud, G., Mgret, R., Giremus, A., Berthoumieu, Y. “Discrete extended Kalman filter on Lie groups,” *21st European Signal Processing Conference 2013 (EUSIPCO 2013)*. September, 2013.
- [8] Bourmaud, G., Mégret, R., Arnaudon, M., Giremus, A., “Continuous-Discrete Extended Kalman Filter on Matrix Lie Groups Using Concentrated Gaussian Distributions,” *Journal of Mathematical Imaging and Vision*, 1-20. 2014.
- [9] Chirikjian, G.S., *Stochastic Models, Information Theory, and Lie Groups: Volume 2 - Analytic Methods and Modern Applications*, Birkhäuser, December 2011.
- [10] Chirikjian, G.S., Kyatkin, A.B., Engineering Applications of Noncommutative Harmonic Analysis, CRC Press, October 2000.
- [11] Citti, G., Sarti, A., “A Cortical Based Model of Perceptual Completion in the Roto-Translation Space,” *J. Math. Imaging and Vision*, 24(3):307326, 2006.
- [12] Duits, R., van Almsick, M., Duits, M., Franken, E., Florack, L.M.J., “Image processing via shift-twist invariant operations on orientation bundle functions,” in *7th International Conference on Pattern Recognition and Image Analysis: New Information Technologies*, (Niemann Zhuralev et al. Geppener, Gurevich, editors), pp. 193-196, St. Petersburg, October 2004.
- [13] Duits, R., Felsberg, M., Granlund, G., ter Haar Romeny, B., “Image analysis and reconstruction using a wavelet transform constructed from a reducible representation of the Euclidean motion group,” *International Journal of Computer Vision*, 72(1):79-102, 2007.
- [14] Duits, R., Franken, E., “Left-invariant parabolic evolutions on  $SE(2)$  and contour enhancement via invertible orientation scores Part I: Linear left-invariant diffusion equations on  $SE(2)$ ,” *Quart. Appl. Math.*, 68:255-292, 2010.
- [15] Zhang, J., Duits, R., Romeny, B.M., “On Numerical Approaches for Linear Left-invariant Diffusions on  $SE(2)$ , their Comparison to Exact Solutions, and their Applications in Retinal Imaging,” arXiv preprint arXiv:1403.3320, 2014.
- [16] Hoffman, W.C., “Higher visual perception as prolongation of the basic Lie transformation group,” *Mathematical Biosciences*, 6:437-471, 1970.
- [17] Long, A., Wolfe, K.C., Mashner, M., Chirikjian, G.S., “The Banana Distribution is Gaussian: A Localization Study with Exponential Coordinates.” *Robotics: Science and Systems*, (2012).
- [18] Kwon, J., Choi, M., Park, F.C., Chun, C., “Particle filtering on the Euclidean group: framework and applications,” *Robotica*, 25(6):725-737, 2007.
- [19] Mahony, R., Kumar, V., Corke, P., “Multirotor aerial vehicles: Modeling, estimation, and control of quadrotor,” *IEEE Robotics and Automation Magazine* 19(3):20-32, 2012.
- [20] Miller, L.M., Murphey, T.D., “Trajectory optimization for continuous ergodic exploration on the motion group  $SE(2)$ ,” in *52nd Annual IEEE Conference on Decision and Control (CDC 2013)*, pp. 4517-4522, December, 2013.
- [21] Mumford, D., “Elastica and computer vision,” in *it Algebraic Geometry and Its Applications*, Chandrajit Bajaj (Ed.), Springer-Verlag: New York, 1994.
- [22] Park, F.C., *The Optimal Kinematic Design of Mechanisms*, Ph.D. Thesis, Division of Engineering and Applied Sciences, Harvard University, Cambridge, MA 1991.
- [23] Park, W., Kim, J.S., Zhou, Y., Cowan, N.J., Okamura, A.M., Chirikjian, G.S., “Diffusion-based motion planning for a non-holonomic flexible needle model,” *Proceedings of the IEEE Int. Conf. on Robotics and Automation*, Barcelona, Spain, April 2005, pp. 4600-4605.
- [24] Park, W., Liu, Y., Zhou, Y., Moses, M., Chirikjian, G.S., “Kinematic State Estimation and Motion Planning for Stochastic Nonholonomic Systems Using the Exponential Map,” *Robotica*, 26(4), 419-434. July- August 2008
- [25] Piggott, M.J., Solo, V., “Stochastic Numerical Analysis For Brownian Motion On  $SO(3)$ ,” 53rd IEEE Conference on Decision and Control December 15-17, 2014. Los Angeles, California, USA 3420-3425
- [26] Smith,P., Drummond, T., and Roussopoulos, K., “Computing MAP trajectories by representing, propagating and combining pdfs over groups,” *Proceedings of the 9th IEEE International Conference on Computer Vision*, volume II, pages 1275-1282, Nice, 2003.
- [27] Su, S., Lee, C.S.G., “Manipulation and Propagation of Uncertainty and Verification of Applicability of Actions in assembly Tasks,” *IEEE Transactions on Systems, Man, and Cybernetics*, Vol. 22, No. 6, p. 1376-1389, 1992.
- [28] Thrun, S., Burgard, W., Fox, D., *Probabilistic Robotics*, MIT Press, Cambridge, MA, 2005.
- [29] Wang, Y., Chirikjian, G.S., “Error Propagation on the Euclidean Group with Applications to Manipulator Kinematics,” *IEEE Transactions on Robotics*, 22(4):591-602 August 2006.
- [30] Wang, Y., Zhou, Y., Maslen, D. K., Chirikjian, G.S., “Solving phase-noise Fokker-Planck equations using the motion-group Fourier transform,” *IEEE Transactions on Communications*, 54(5):868-877, 2006.
- [31] Williams, L.R., Jacobs, D.W., “Stochastic completion fields: A neural model of illusory contour shape and salience,” *Neural Computation*, 9(4):837858, 1997.
- [32] Williams, L.R., Jacobs, D.W., “Local Parallel Computation of Stochastic Completion Fields,” *Neural Computation*, 9(4):859881, 1997.
- [33] Wolfe, K.C., Chirikjian, G.S., “Signal Detection on Euclidean Groups: Applications to DNA Bends, Robot Localization, and Optical Communication,” *IEEE Journal of Selected Topics in Signal Processing* 7(4):708-719, 2013.
- [34] Zhou, Y., Chirikjian, G.S., “Probabilistic Models of Dead-Reckoning Error in Nonholonomic Mobile Robots,” *ICRA'03*, Taipei, Taiwan, September, 2003, pp. 1594-1599.
- [35] Zweck, J., Williams, L.R., “Euclidean Group Invariant Computation of Stochastic Completion Fields Using Shiftable-Twistable Functions,” *Journal of Mathematical Imaging and Vision*, 21: 135154, 2004